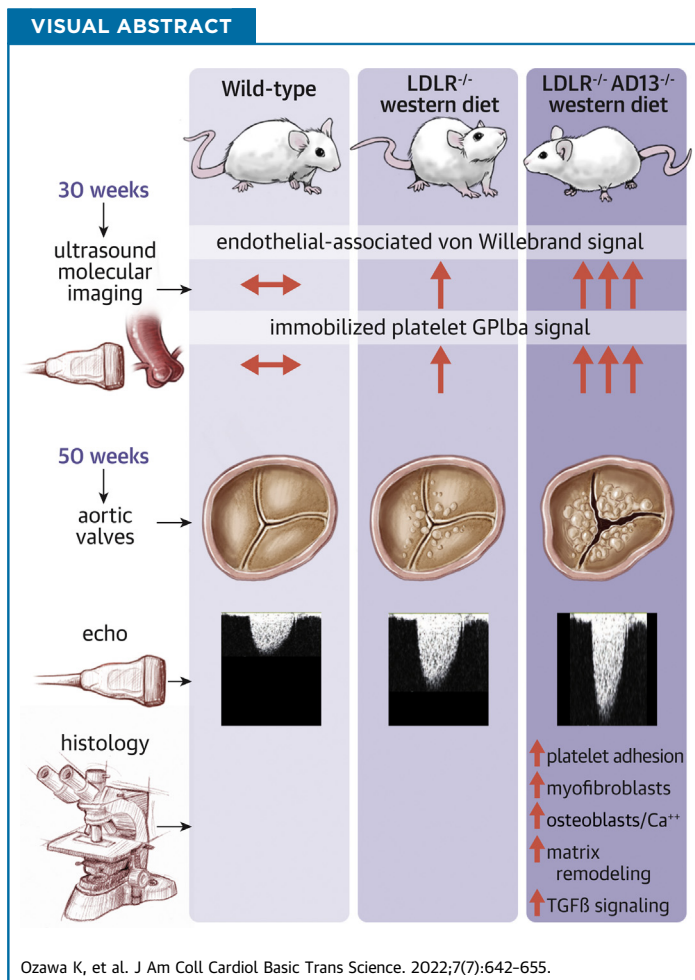


ORIGINAL RESEARCH - PRECLINICAL

Reduced Proteolytic Cleavage of von Willebrand Factor Leads to Aortic Valve Stenosis and Load-Dependent Ventricular Remodeling



Koya Ozawa, MD, PhD,^a Matthew A. Muller, BA,^a Oleg Varlamov, PhD,^b Matthew W. Hagen, PhD,^a William Packwood, BS,^a Terry K. Morgan, MD, PhD,^{c,d} Aris Xie, MS,^a Claudia S. López, PhD,^d Dominic Chung, PhD,^e Junmei Chen, PhD,^e José A. López, MD,^e Jonathan R. Lindner, MD^{a,b}



HIGHLIGHTS

- Excess vWF on the aortic valve surface predisposes to AS.
- Valvular vWF likely promotes AS through myofibroblastic and osteogenic pathways known to be stimulated by platelet-derived factors.
- Effects of excess endothelial vWF also cause arterial noncompliance, resulting in rapid progression of pressure-related ventricular remodeling.

SUMMARY

We hypothesized that excess endothelial-associated von Willebrand factor (vWF) and secondary platelet adhesion contribute to aortic valve stenosis (AS). We studied hyperlipidemic mice lacking ADAMTS13 (*LDLR*^{-/-}*AD13*^{-/-}), which cleaves endothelial-associated vWF multimers. On echocardiography and molecular imaging, *LDLR*^{-/-}*AD13*^{-/-} compared with control strains had increased aortic endothelial vWF and platelet adhesion and developed hemodynamically significant AS, arterial stiffening, high valvulo-aortic impedance, and secondary load-dependent reduction in LV systolic function. Histology revealed leaflet thickening and calcification with valve interstitial cell myofibroblastic and osteogenic transformation, and evidence for TGFβ1 pathway activation. We conclude that valve leaflet endothelial vWF-platelet interactions promote AS through juxtacrine platelet signaling. (J Am Coll Cardiol Basic Trans Science 2022;7:642-655) © 2022 The Authors. Published by Elsevier on behalf of the American College of Cardiology Foundation. This is an open access article under the CC BY-NC-ND license (<http://creativecommons.org/licenses/by-nc-nd/4.0/>).

ABBREVIATIONS AND ACRONYMS

AS = aortic valve stenosis
MMP = matrix metalloproteinase
PMV = platelet microvesicles
pSMAD2 = phosphorylated SMAD2
TGF = transforming growth factor
VEC = valvular endothelial cell
VIC = valvular interstitial cell
vWF = von Willebrand factor
WSD = Western-style diet

Aortic valve stenosis (AS) occurs from a broad array of processes including the generation of reactive oxygen species, cytokine and growth factor signaling, abnormal regulation of extracellular matrix content, and osteogenic signaling.^{1,2} This knowledge has not translated to any successful medical therapy to slow AS progression in patients, largely because the modifiable triggers that initiate and promote progression of AS are incompletely understood.

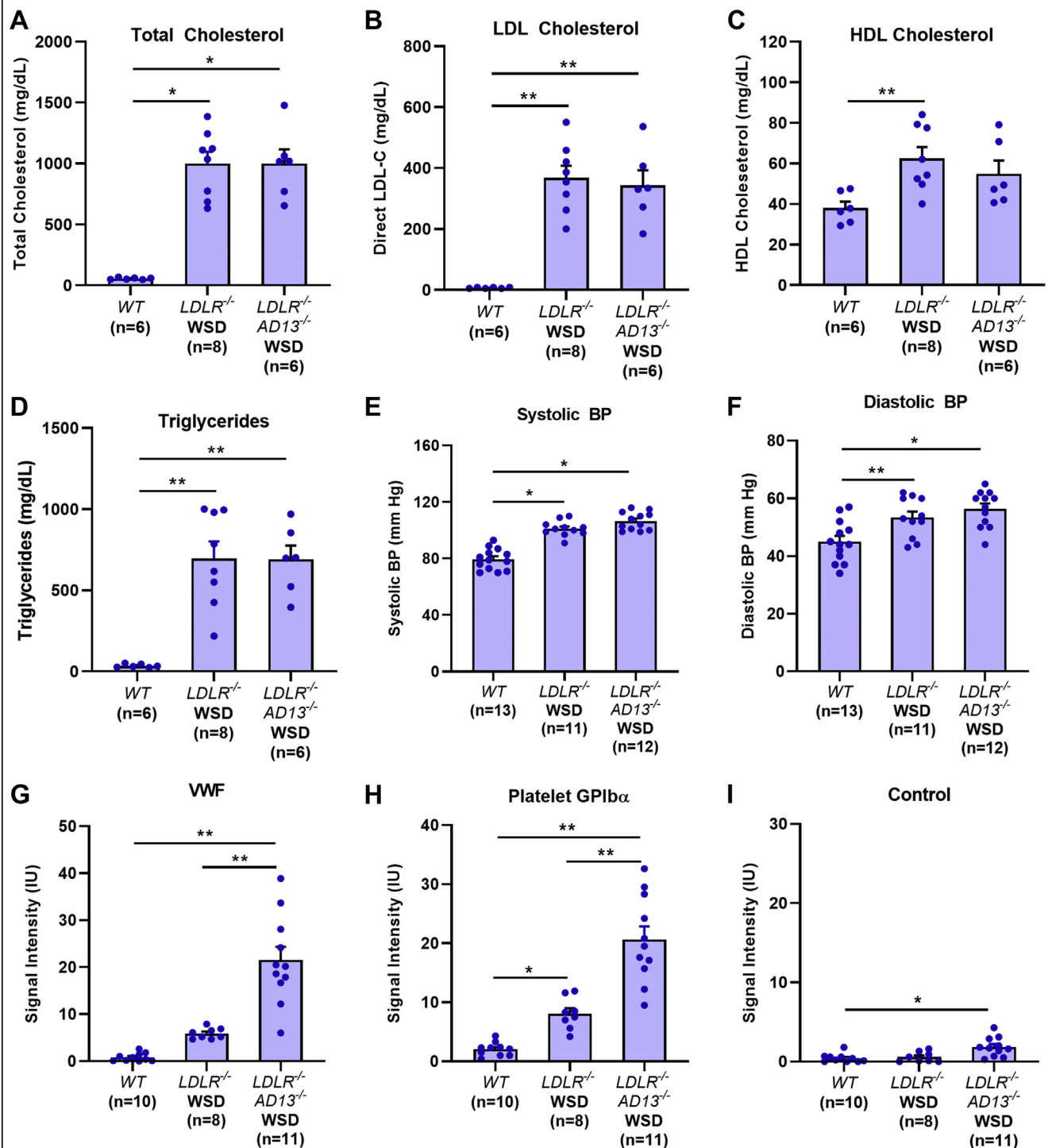
Platelets are a source of growth factors, chemokines, and cytokines that can potentially alter the cellular and matrix composition of heart valves. Yet, the role of platelets in AS is uncertain. In humans, associations between platelet activation and severity of AS are modest, and may not reflect a pathogenic role of platelets but rather the effect of valve shear on platelet activation.³ Moreover, the activation status of circulating platelets does not reflect their full pathogenic potential. Platelet adhesion mediated by interaction of constitutively-expressed glycoprotein-Ibα (GPIbα) component of the GPIb/V/IX complex, and endothelial-associated von Willebrand Factor (vWF) can activate vascular cells through chemokine and growth factor signaling and inflammasome activation.⁴⁻⁷ These processes have been recognized to be proatherogenic.^{8,9} Shear-mediated self-association of vWF and exposure of the A1 binding domain for platelet GPIbα could similarly contribute to AS

through platelet binding and juxtacrine or paracrine signaling through factors such as transforming growth factor-β1 (TGFβ1) that are known to cause myofibroblastic or osteogenic activation of valvular cells.^{10,11} Platelet adhesion to the surface of aortic leaflets has been described in mice with hyperlipidemia and on explanted leaflets from humans with AS.^{12,13} Moreover, platelet-specific deficiency of TGFβ1 has been shown to reduce aortic valve thickening in hyperlipidemic mice,¹² and activated platelet products have been shown to produce pro-osteogenic profiles of cultured valve interstitial cells (VICs).¹³

In the current study, we hypothesized that excess endothelial-associated vWF contributes to not only aortic valve thickening, but also the development of AS through leaflet adhesion of platelets or platelet microvesicles (PMVs) and subsequent myofibroblastic and osteogenic transformation of VICs. We studied mice with hyperlipidemia produced by Western-style diet (WSD) and genetic deficiency of the low-density lipoprotein receptor (*LDLR*^{-/-}) that were also deficient for ADAMTS-13, the enzyme responsible for proteolytic cleavage and removal of ultra-large self-associated multimers of vWF from the endothelial surface.¹⁴ Comprehensive noninvasive in vivo imaging data were integrated with tissue histology to examine the effect of excess valve endothelial cell (VEC) vWF on leaflet platelet adhesion, aortic valve morphology, VIC transformation, valve

From the ^aKnight Cardiovascular Institute, Oregon Health & Science University, Portland, Oregon, USA; ^bOregon National Primate Research Center, Oregon Health & Science University, Portland, Oregon, USA; ^cDepartment of Pathology, Oregon Health & Science University, Portland, Oregon, USA; ^dDepartment of Biomedical Engineering, Oregon Health & Science University, Portland, Oregon, USA; and the ^eBloodWorks NW, Seattle, Washington, USA.

The authors attest they are in compliance with human studies committees and animal welfare regulations of the authors' institutions and Food and Drug Administration guidelines, including patient consent where appropriate. For more information, visit the [Author Center](#).

FIGURE 1 Characterization of the Murine Models at Age 30 Weeks

(A to D) Mean \pm SEM plasma lipid concentrations including total cholesterol, LDL cholesterol, HDL cholesterol, and triglycerides. (E and F) Mean \pm SEM systolic and diastolic awake blood pressure (BP) measurements. (G and I) Mean \pm SEM signal intensity on contrast ultrasound molecular imaging signal from the aortic root for endothelial-associated vWF by microbubble targeting of the A1 binding domain, platelet adhesion by targeting GPIb α , and control microbubble contrast agent. *P* values are adjusted for multiple comparisons. Examples of contrast ultrasound molecular imaging of the aortic root from all 3 murine groups are illustrated in Supplemental Figure 1. **P* < 0.05; ***P* < 0.001 (adjusted). HDL = high-density lipoprotein; LDL = low-density lipoprotein; vWF = von Willebrand factor; WSD = Western-style diet; WT = wild type.

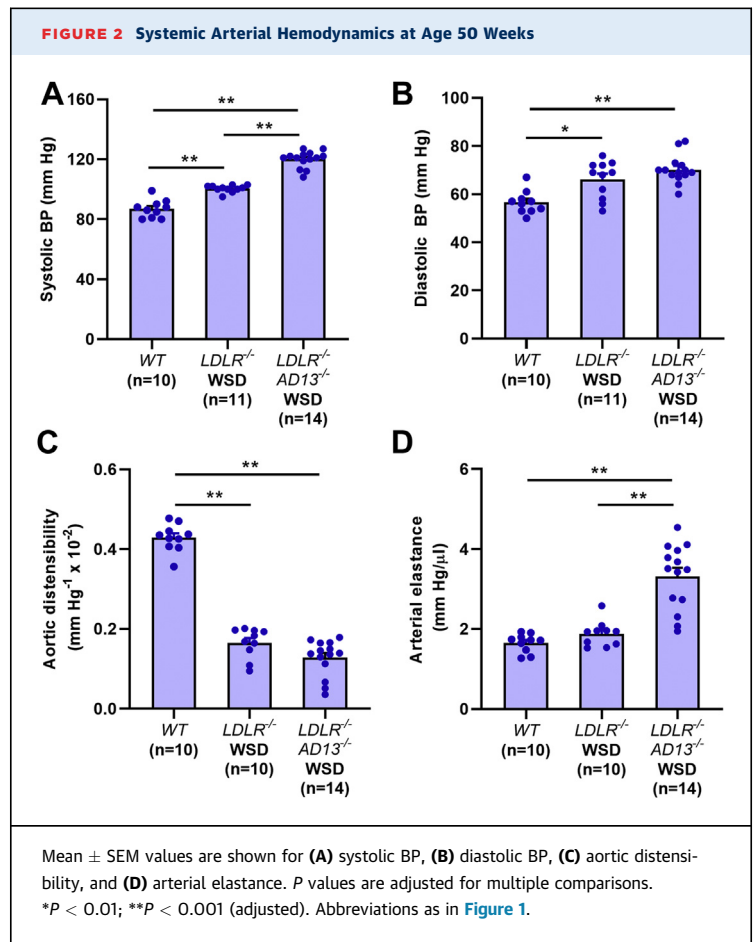
hemodynamics, and load-dependent changes of the left ventricle (LV).

METHODS

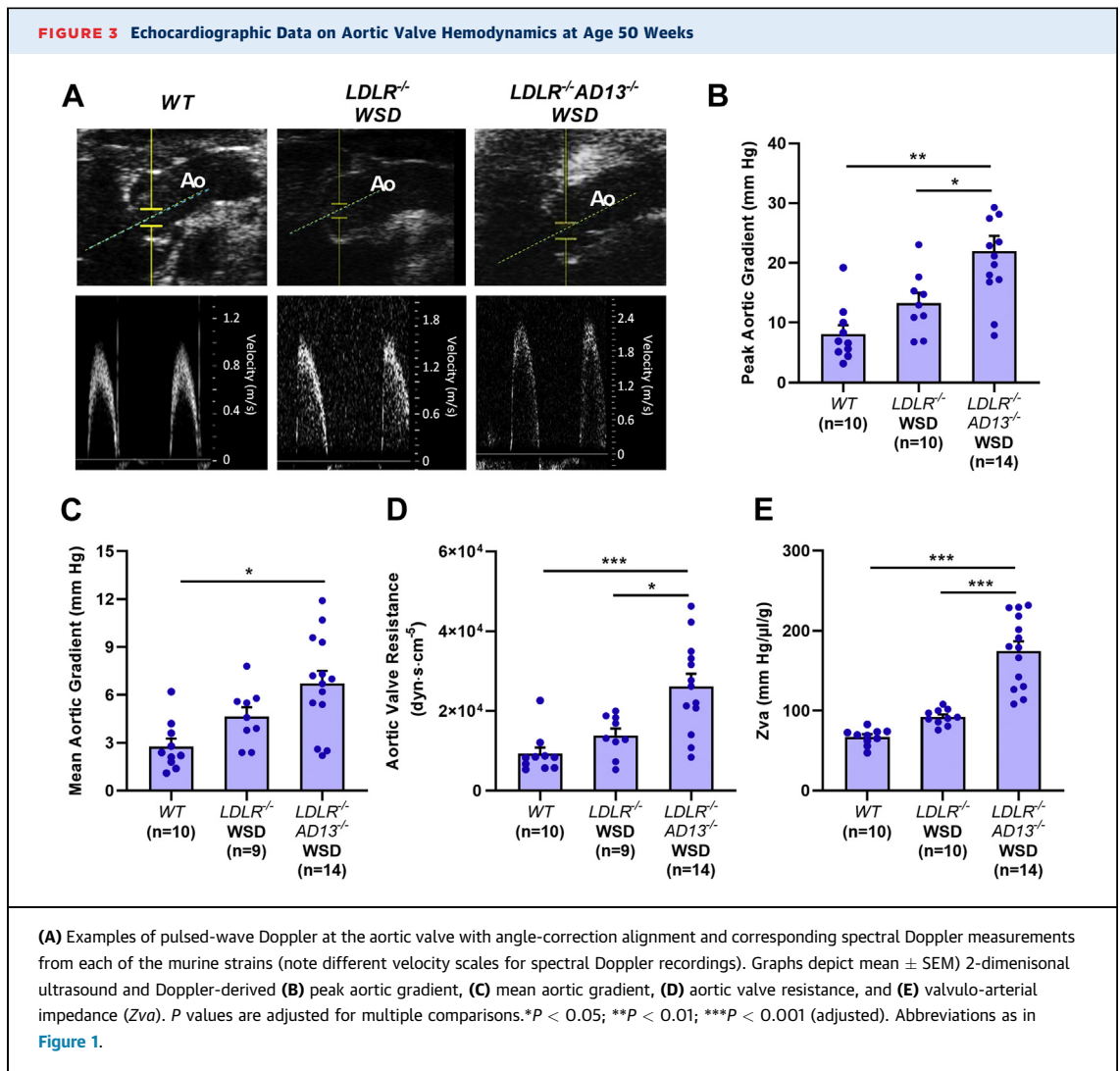
A detailed description of all methods is provided in the [Supplemental Appendix](#). A general description of study design follows. The study was approved by the Animal Care and Use Committee of the Oregon Health & Science University. We studied wild-type C57BL/6 mice, *LDLR*^{-/-} mice on a C57BL/6 background, and *LDLR*^{-/-} mice deficient for *ADAMTS13* (*LDLR*^{-/-}*AD13*^{-/-}) generated by crossing *LDLR*^{-/-} mice with *AD13*^{-/-} mice. At age 14 weeks, *LDLR*^{-/-} and *LDLR*^{-/-}*AD13*^{-/-} mice were switched from chow diet to WSD containing 21% fat by weight (15% saturated fat), representing 42% of caloric intake. At age 50 weeks, comprehensive ultrasound evaluation of aortic hemodynamics and LV structure and function was performed, and plasma vWF and ADAMTS13 activity were measured. Also at 50 weeks, histological evaluation of the aortic valve and aorta by light microscopy, immunofluorescence, and transmission electron microscopy was performed for characterization of valve leaflet thickening, leaflet vWF, platelet adhesion, matrix and matrix metalloproteinase-9 (MMP-9), calcification, VIC myofibroblastic transformation, phosphorylated SMAD2 (pSMAD2) and β-catenin as a marker of TGFβ1 signaling, and myocyte hypertrophy. In situ hybridization with RNA-scope was performed for transcriptomic increases in osteocalcin as a marker for osteogenic transformation. Computed tomography angiography was performed for coronary anatomy. At 30 weeks of age, representing a midpoint between initiation of WSD and final evaluation, the intended phenotype for the murine groups was evaluated by measurement of plasma lipids, complete blood counts, ultrasound molecular imaging of platelet adhesion and endothelial-associated vWF, and histology for vWF.

RESULTS

ABNORMAL ENDOTHELIAL PHENOTYPE AND HYPERTENSION IN MICE LACKING ADAMTS13. Plasma lipids, blood pressure, and endothelial molecular imaging were performed at age 30 weeks, selected as an intermediate time point between initiation of WSD and the final evaluation of valve status to assess differences between the murine strains during disease development. At this age, *LDLR*^{-/-} and *LDLR*^{-/-}*AD13*^{-/-} mice on WSD had similar degrees of hyperlipidemia compared with wild-type mice, manifesting



as elevated total cholesterol, LDL cholesterol, non-LDL/high-density lipoprotein cholesterol, and triglycerides ([Figures 1A to 1D](#)). Awake systolic and diastolic blood pressure were elevated in both *LDLR*^{-/-} and *LDLR*^{-/-}*AD13*^{-/-} mice on WSD compared with wild-type mice ([Figures 1E and 1F](#)). Contrast ultrasound molecular imaging of the aortic root was performed using validated protocols with microbubble probes that remain entirely within the vascular compartment and that detect endothelial-associated vWF by targeting the shear-exposed A1 domain binding domain, and platelet adhesion by targeting GPIbα of the GPIb-V-IX complex.^{15,16} Both *LDLR*^{-/-} and *LDLR*^{-/-}*AD13*^{-/-} mice on WSD had higher signal compared with wild-type mice for endothelial-associated vWF A1 domain and platelet GPIbα, and the signal for both of these targets was 2- to 3-fold higher in *LDLR*^{-/-}*AD13*^{-/-} mice than *LDLR*^{-/-} mice ([Figures 1G to 1I, Supplemental Figure 1](#)). Molecular imaging data for vWF were corroborated by immunofluorescent histology at age 30 weeks showing enhanced endothelial vWF



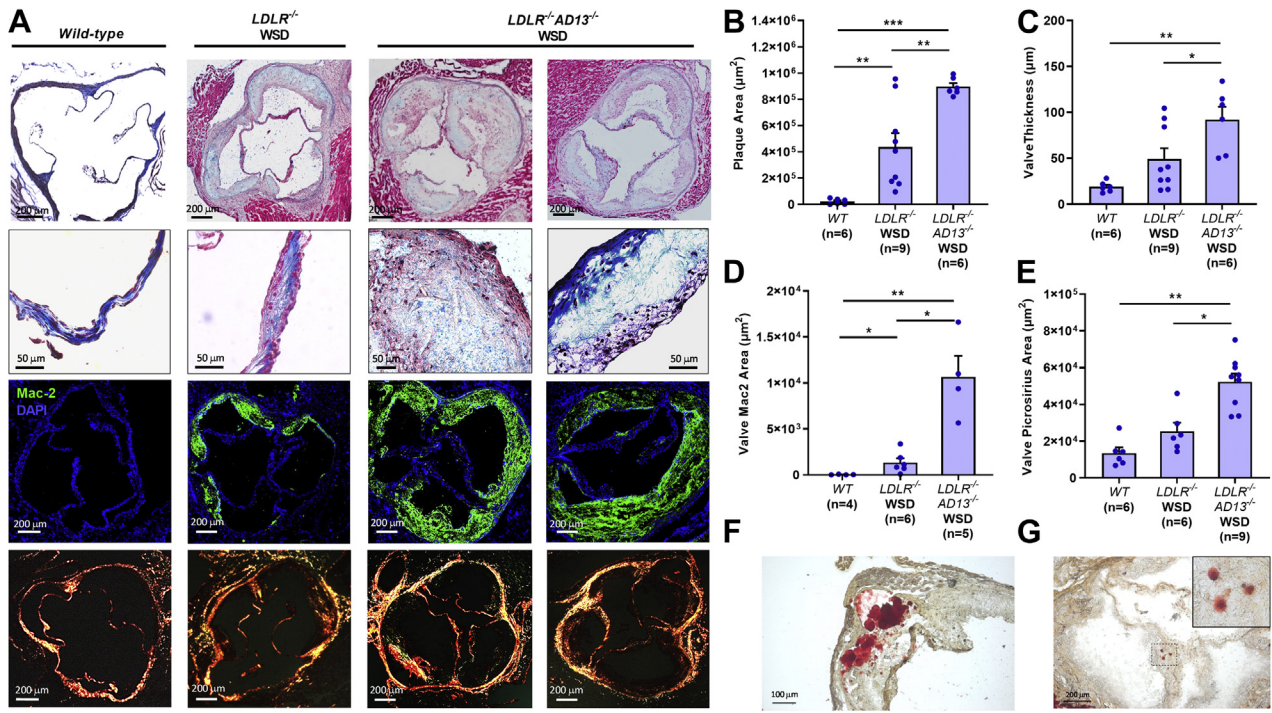
not only in regions of plaque formation in the aortic sinuses, but also on both the ventricularis and fibrosa (aortic) aspects of the aortic valve leaflets (Supplemental Figure 2).

ADAMTS13 ACTIVITY, CIRCULATING vWF, AND PLATELET COUNT. At 50 age weeks, group-wise differences in plasma ADAMTS13 activity and vWF concentration were evaluated (Supplemental Table 1). Results were similar between wild-type and *LDLR^{-/-}* mice on WSD; whereas *LDLR^{-/-}AD13^{-/-}* mice uniformly had no detectable ADAMTS13 activity and had significantly lower circulating plasma vWF concentrations compared with the other groups, a finding that is consistent with impaired ability to proteolytically cleave vWF from the endothelial surface and into the circulating plasma pool. Platelet counts

tended to be higher in *LDLR^{-/-}AD13^{-/-}* mice, although this did not meet statistical significance (Supplemental Table 1).

BLOOD PRESSURE AND AORTIC MECHANICAL PROPERTIES AT AGE 50 WEEKS. At 50 age weeks, aortic hemodynamics were again assessed to fully evaluate the combined hemodynamic influence of blood pressure, vascular stiffness, and aortic valve disease in the different strains. Awake systolic and diastolic BP were higher in *LDLR^{-/-}* and *LDLR^{-/-}AD13^{-/-}* mice on WSD compared with wild-type mice (Figures 2A and 2B). Systolic BP was highest in *LDLR^{-/-}AD13^{-/-}* mice. Aortic distensibility (Figure 2C), representing the aortic strain-pressure relation, was reduced for *LDLR^{-/-}* and *LDLR^{-/-}AD13^{-/-}* mice on WSD compared with wild-type mice. Differences in

FIGURE 4 Aortic Valve Histology at Age 50 Weeks



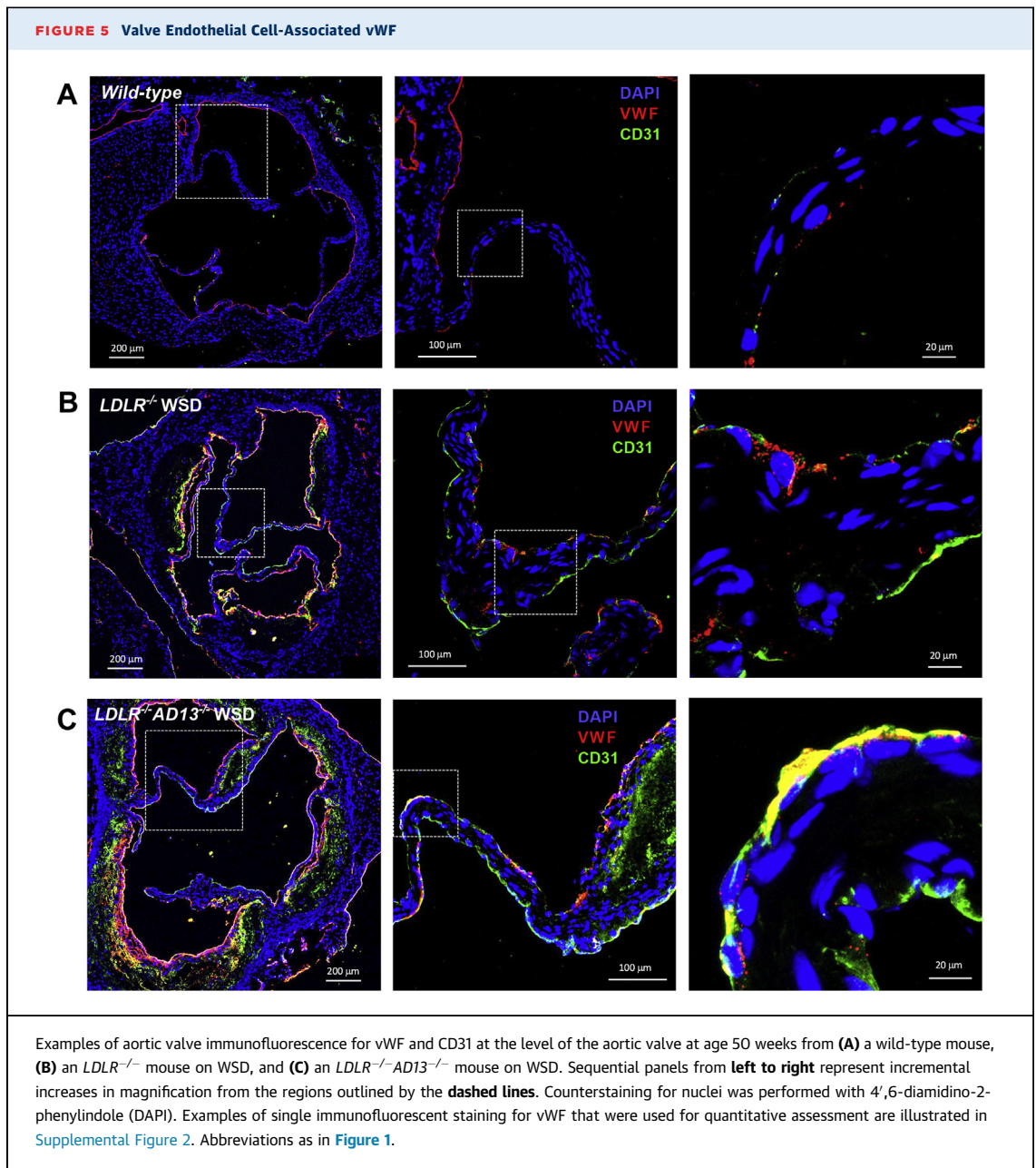
(A) Examples of aortic root histology at the level of the valve for wild-type mouse, *LDLR*^{-/-} mouse on WSD, and 2 different *LDLR*^{-/-}*AD13*^{-/-} mice on WSD at age 50 weeks illustrating Masson's trichrome at low and high magnification (top 2 rows), Mac-2 (galectin-3) immunofluorescence with positive staining in the green fluorescent range (third row), and picosirius red staining visualized under polarized light (bottom row). Quantitative microscopy data (mean ± SEM) are provided for measurement of (B) plaque area, (C) average valve thickness, (D) valve leaflet area with positive Mac-2 staining, and (E) valve leaflet area with positive picosirius staining. *P* values are adjusted for multiple comparisons. Alizarin red staining of the leaflets from *LDLR*^{-/-}*AD13*^{-/-} mice showing (F) dense focal calcific nodules in the body of the leaflet; and (G) low-intensity staining of individual VICs (low magnification image of the leaflets shown, with inset illustrating high magnification of the area denoted by the dashed lines). **P* < 0.05; ***P* < 0.01; ****P* < 0.001 (adjusted). Abbreviations as in Figure 1.

aortic distensibility between *LDLR*^{-/-} and *LDLR*^{-/-}*AD13*^{-/-} mice did not reach statistical significance (adjusted *P* = 0.07). Arterial elastance, which takes into account differences in stroke volume and reflects nonpulsatile load and arterial compliance,¹⁷ was significantly higher in *LDLR*^{-/-}*AD13*^{-/-} mice compared with the other strains, consistent with increased peripheral arterial afterload (Figure 2D).

HEMODYNAMIC AORTIC VALVE STENOSIS OCCURS IN *LDLR*^{-/-}*AD13*^{-/-} mice. On echocardiography at 50 age weeks, there was a stepwise increase in peak and mean aortic gradients between wild-type *LDLR*^{-/-} mice on WSD and *LDLR*^{-/-}*AD13*^{-/-} mice on WSD, although differences between *LDLR*^{-/-} and *LDLR*^{-/-}*AD13*^{-/-} mice did not meet statistical significance only for the mean gradient (Figures 3A to 3C). Compared with other groups, *LDLR*^{-/-}*AD13*^{-/-} mice had significantly greater aortic valve resistance (Figure 3D), which accounts for potential differences

in stroke volume. Valvulo-aortic impedance, reflecting the net afterload placed on the LV from both aortic valve resistance and systolic hypertension, was 2- to 3-fold higher in *LDLR*^{-/-}*AD13*^{-/-} mice compared with the other groups (Figure 3E). Doppler studies did not detect more than trivial to mild aortic regurgitation in any animal.

AORTIC LEAFLET MORPHOLOGY, ENDOTHELIAL-ASSOCIATED vWF, AND PLATELET ADHESION. Histology at age 50 weeks revealed plaque that was rich in Mac-2 staining in the aortic sinuses in both *LDLR*^{-/-} and *LDLR*^{-/-}*AD13*^{-/-} mice on WSD (Figure 4A). In *LDLR*^{-/-}*AD13*^{-/-} mice, plaque often extended into the base of the leaflets. Plaque-like structures on the leaflets were also observed in some animals. On quantitative analysis, *LDLR*^{-/-}*AD13*^{-/-} mice had 2-fold greater aortic sinus plaque than *LDLR*^{-/-} mice (Figure 4B). Valve thickening by Masson's trichrome staining was present in both *LDLR*^{-/-} and *LDLR*^{-/-}*AD13*^{-/-} mice,

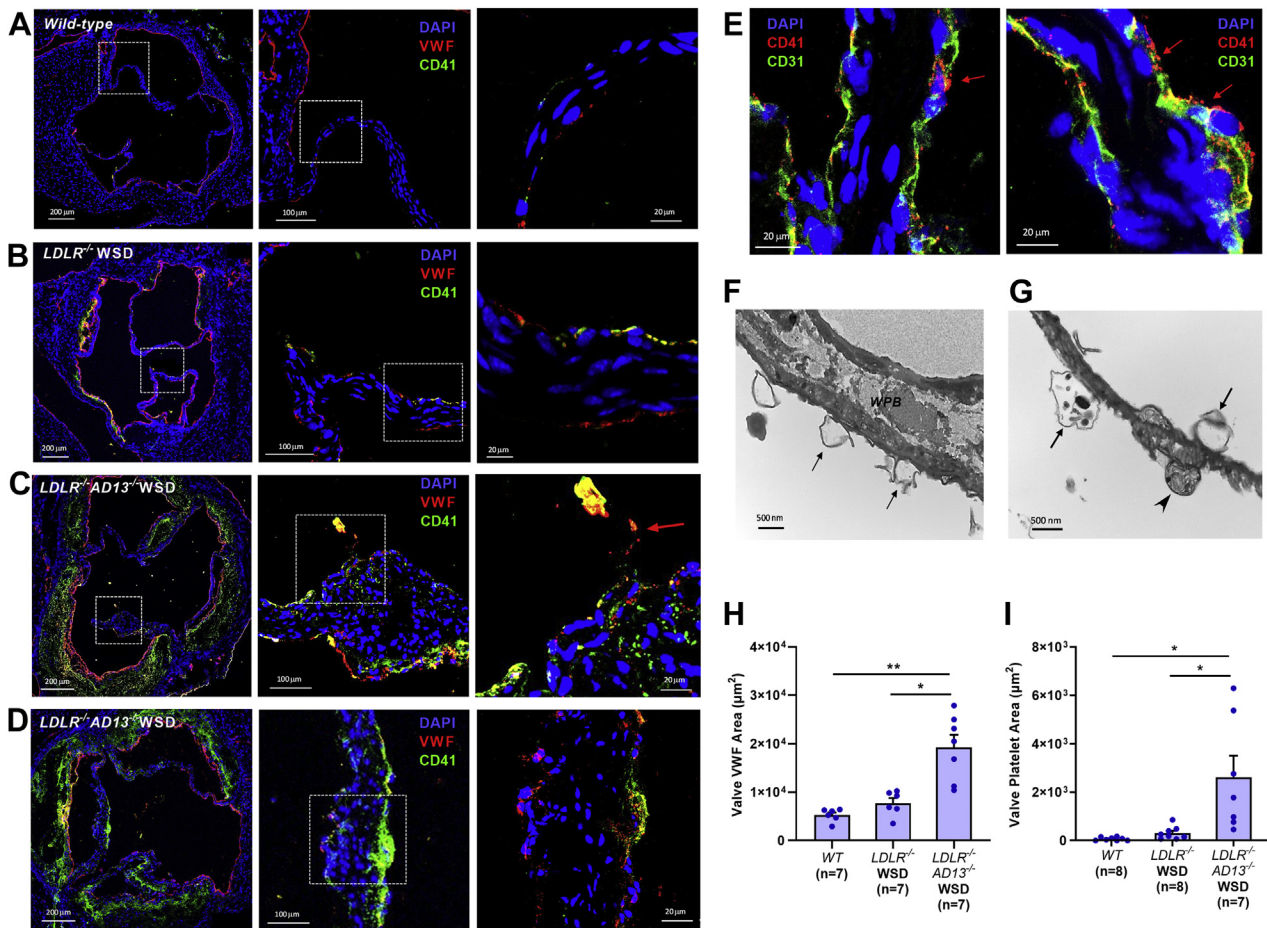


but was far greater in $LDLR^{-/-}AD13^{-/-}$ mice in which both focal eccentric thickening and diffuse thickening were observed (Figures 4A and 4C). Leaflet thickening was associated with disarray of the normal laminar organized layers, a transmural increase in valve matrix including collagen, and increases in valve cellularity and area staining for Mac-2 (Figures 4A, 4D, and 4E). The majority of plaque thickening was not from Mac-2-positive plaque-like structures but from the increased matrix and cellularity. On calcium staining with alizarin red, only $LDLR^{-/-}AD13^{-/-}$ mice

exhibited any positive leaflet staining manifest either as dense focal calcific nodules or as lower-intensity staining of VICs consistent with osteogenic transformation (Figures 4F and 4G).¹⁸

On immunofluorescence histology, vWF was observed overlying and within atherosclerotic plaque in the $LDLR^{-/-}$ and $LDLR^{-/-}AD13^{-/-}$ strains as well as on the leaflet surface in all strains, where it was associated with valvular endothelial cells (Figure 5). Qualitatively, in wild-type and $LDLR^{-/-}$ mice, much of the vWF appeared to be within intracellular

FIGURE 6 Platelet Adhesion Patterns at Age 50 Weeks

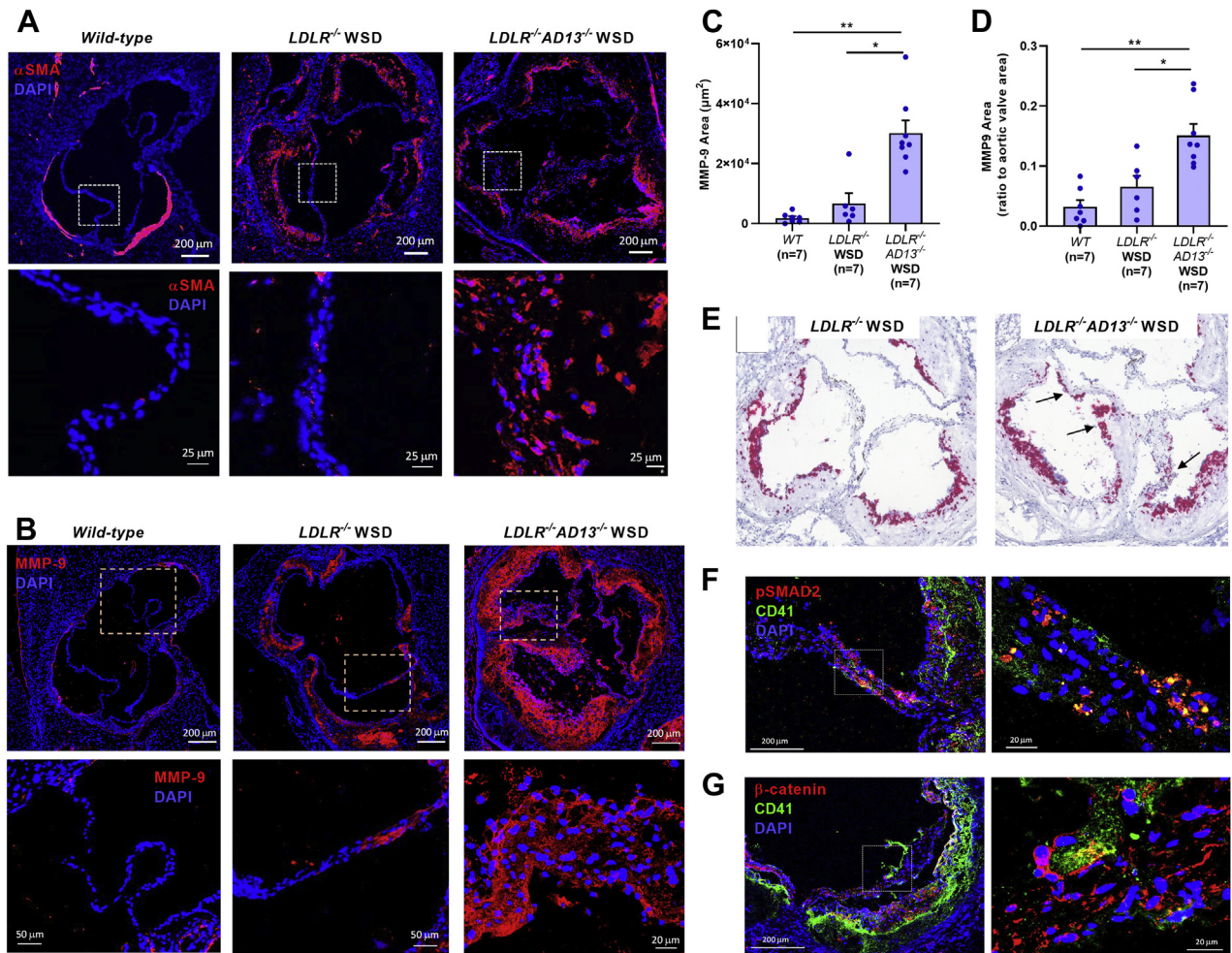


(A to D) Examples of aortic valve dual immunofluorescence for vWF and platelet CD41 at age 50 weeks from (A) a wild-type mouse, (B) an *LDLR*^{-/-} mouse on WSD, and (C and D) 2 separate *LDLR*^{-/-} *AD13*^{-/-} mice on WSD. Sequential panels from left to right represent incremental increases in magnification from the regions outlined by the dashed lines. Red arrow in C indicates evidence for a long vWF multimer on the valve surface with platelets at the distal end (yellow staining indicating dual CD41 and vWF staining). (E) Two examples of aortic valve dual immunofluorescence at high magnification for CD31 and platelet CD41 at age 50 weeks from *LDLR*^{-/-} *AD13*^{-/-} mice on WSD. Arrows indicate the evidence for platelet staining for particles that appear <1 μm in size. (F and G) Transmission electron microscopy showing evidence of extracellular microvesicles (arrows) directly attached to the valvular endothelial cells. The structure denoted by the arrowhead in G may represent either microvesicle with contents but is also consistent with intermediate secretory pods that have been described after Weibel-Palade body (WPB) cell membrane fusion. Graphs depict mean \pm SEM immunofluorescent positive area for (H) valve leaflet vWF and (I) valve leaflet platelet CD41 staining. **P* < 0.01; ***P* < 0.001 (adjusted). Abbreviations as in Figure 1.

granules, consistent with storage in Weibel-Palade bodies (Figures 5A and 5B). The extent of leaflet vWF was greatest in *LDLR*^{-/-} *AD13*^{-/-} mice where it was observed on both the ventricular and aortic aspects of the valve, and often appeared to be nongranular and to be associated with the luminal endothelial surface (Figure 5C). Immunofluorescence for CD41 indicated that there was almost no platelet adhesion to aortic leaflets in wild-type mice, and a modest number of single adhesion events in *LDLR*^{-/-} mice on WSD (Figures 6A and 6B). In *LDLR*^{-/-} *AD13*^{-/-} mice,

the extent of platelet CD41 staining was much greater and was found to be associated with atherosclerotic plaque, with the ventricular and aortic aspects of the aortic valve surface, and in some cases within the interior of the valve (Figures 6C and 6D). Platelets were occasionally observed to be associated with projections of vWF away from the leaflet surface consistent with self-associated ultra-large vWF fibers (Figure 6C). Dual staining revealed that platelet adhesion events occurred primarily at sites of intact endothelium, and not in regions of endothelial

FIGURE 7 Valve Interstitial Cell Myofibroblastic and Osteogenic Transformation

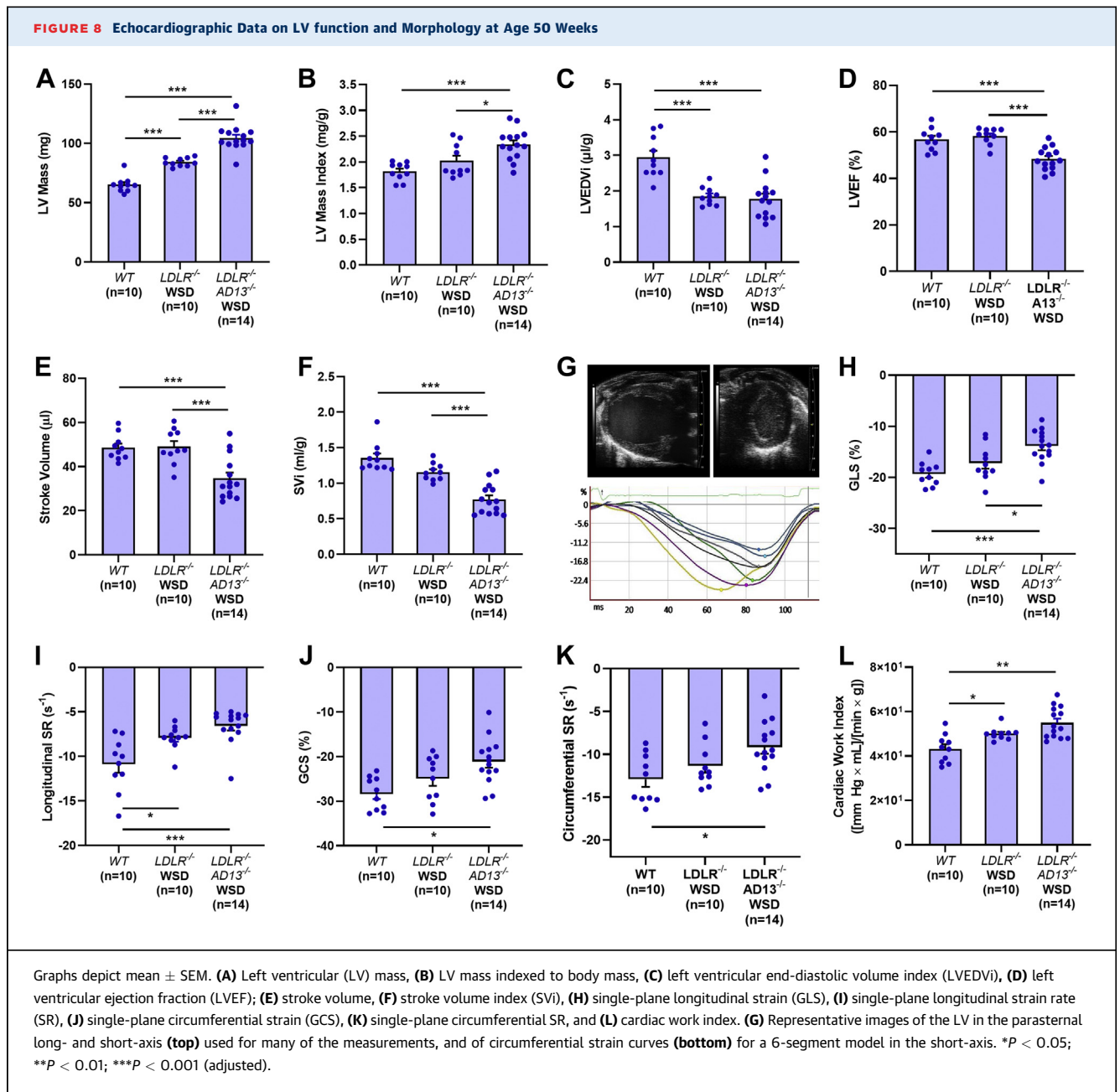


(**A and B**) Examples of aortic valve immunofluorescence for (**A**) α -smooth muscle actin (α SMA) and (**B**) matrix metalloproteinase (MMP)-9 from each murine strain. High-magnification images of the area defined by **dashed lines** are provided **below each image**. Additional examples of α SMA staining are shown in [Supplemental Figure 3](#). Graphs depict mean \pm SEM immunofluorescent-positive area MMP-9 expressed as (**C**) total area and (**D**) proportion of total leaflet area. *P* values are corrected for multiple comparisons. (**D**) In situ hybridization for osteopontin mRNA expression (red staining) illustrating positive staining for aortic plaque in both *LDLR*^{-/-} mice on WSD and *LDLR*^{-/-}*AD13*^{-/-} mice on WSD, but leaflet staining (**arrows**) only in the latter. Examples of dual immunofluorescent staining for: (**E**) pSMAD2 and platelet CD41, and (**F**) β -catenin and platelet CD41 from *w LDLR*^{-/-}*AD13*^{-/-} mice on WSD, with high-magnification images shown to the right. Additional examples from all 3 strains are shown in [Supplemental Figure 4](#). **P* < 0.01; ***P* < 0.001 (adjusted). Abbreviations as in [Figure 1](#).

erosion ([Figure 6E](#)). Many of the CD41-positive entities seen on high-magnification imaging appeared submicron in size, consistent with adhesion of not only platelets but also PMVs. This finding was corroborated by transmission electron microscopy of valve tissue from *LDLR*^{-/-}*AD13*^{-/-} mice, which detected that vesicles that were \approx 400 nm in diameter were observed attached to valve endothelial cells ([Figures 6F and 6G](#)). On quantitative assessment, valvular vWF and valve-associated CD41-positive

platelet or PMV staining was greatest in *LDLR*^{-/-}*AD13*^{-/-} mice on WSD ([Figures 6H and 6I](#)).

DISEASE-RELATED CHANGES IN AORTIC VALVE INTERSTITIAL CELLS AND ENDOTHELIAL CELLS. Because platelets contain factors that are recognized to directly or indirectly induce myofibroblastic transformation of VICs, immunofluorescence was performed for α -smooth muscle actin (SMA) as a marker of myofibroblastic transformation.^{10,12,19} The number of cells positive for alpha smooth cell actin



(α SMA) and the intensity of staining were both greater in $LDLR^{-/-}AD13^{-/-}$ mice (Figure 7A, Supplemental Figure 3). The α SMA-positive VICs were largely responsible for the increase in cellularity seen on Masson's trichrome staining. Staining for MMP-9, a marker for active matrix remodeling that has been associated with progressive AS in humans and with myofibroblastic VICs,²⁰ was intense within the leaflets of $LDLR^{-/-}AD13^{-/-}$ mice, particularly in areas with focal valve thickening (Figures 7B to 7D). In situ hybridization for osteopontin (*SPP1*) transcription

as a marker for the early stages of VIC osteogenic transformation²¹ revealed dense transcription in aortic sinus plaques for both $LDLR^{-/-}$ and $LDLR^{-/-}AD13^{-/-}$ mice. However, leaflet staining was only observed only in $LDLR^{-/-}AD13^{-/-}$ mice (Figure 7E). Osteopontin was not seen in any wild-type mice.

Histologic evaluation was performed for pSMAD2 and for β -catenin as a marker for activation of the canonical Wnt pathway. These represent 2 separate signaling pathways that have been thought to contribute to aortic valve disease and VIC

myofibroblastic differentiation through TGF β 1 signaling.^{10,12,19} The intensity and extent of expression for both pSMAD2 and β -catenin was greater in *LDLR*^{-/-}*AD13*^{-/-} mice than other groups, and both markers were present in VICs and VECs (Figures 7F and 7G, Supplemental Figure 4). Platelets also occasionally were found to express pSMAD2. The percentage of β -catenin staining in *LDLR*^{-/-}*AD13*^{-/-} mice that was nuclear in location was $23 \pm 9\%$. Staining of VECs and VICs for both pSMAD2 and β -catenin was often spatially associated with regions where there was also platelet or PMV adhesion on CD41 staining. Staining for NOTCH-1 was present in all strains but was similar between strains (Supplemental Figure 5).

LOAD-DEPENDENT CHANGES IN LV FUNCTION. On echocardiography, *LDLR*^{-/-}*AD13*^{-/-} mice on WSD had increased LV mass and smaller LV end-diastolic volumes (Figures 8A to 8C). In *LDLR*^{-/-}*AD13*^{-/-} mice, indexes of systolic function that are known to be afterload-dependent were all impaired including LV ejection fraction, SV, SVi, global longitudinal and circumferential strain, and strain rate (Figures 8D to 8K). Because increased contractility is a compensatory mechanism for maintaining cardiac output in response to increased impedance,¹⁷ cardiac work was evaluated and found to be highest in the *LDLR*^{-/-}*AD13*^{-/-} mice on WSD (Figure 8L), arguing against a decompensated state. Because *LDLR*^{-/-}*AD13*^{-/-} mice on WSD had a far greater degree of aortic plaque formation, coronary computed tomography angiography was performed to exclude obstructive coronary artery disease as a cause for reduced LV ejection fraction and stroke volume. These studies failed to detect any epicardial coronary stenosis (Supplemental Figure 6).

DISCUSSION

The primary aim of this study was to examine how reduced proteolytic cleavage of vWF contributes to the development of AS. vWF is a large, multimeric glycoprotein involved in hemostasis that is synthesized by endothelial cells and megakaryocytes. Much of the vWF secreted by endothelial cells remains associated with the endothelial luminal surface in large self-associated form until it is removed by ADAMTS13.²² High fluid shear stress results in conformational change of vWF, thereby exposing the A1 domain, which mediates binding to platelet GPIIb/IIIa, and also the otherwise cryptic A2 domain for ADAMTS13-mediated proteolysis or self-association.^{14,23} Failure of the proteolytic process, which can occur from a variety of acquired causes including

oxidative stress and lipid disorders,^{15,24} leads to excess self-associated vWF on the endothelial surface. Subsequent platelet adhesion to vWF in areas of high shear is known to influence vascular tissues through the direct recruitment of innate immune cells, release of platelet-derived signaling molecules, and membrane transfer of adhesion molecules or chemokines from platelets to other cells.^{4,5,25}

The underlying hypothesis that excess endothelial-associated vWF and secondary platelet adhesion accelerates aortic valve thickening was based on several lines of reasoning. Development of AS involves a cascade of cellular and matrix events including inflammatory activation as well as growth factor and osteogenic signaling through a wide variety of pathways that induce myofibroblastic and osteoblastic transformation of VICs.^{1,2,19,26} Platelets have the potential to stimulate these processes through either the recruitment of inflammatory cells, or signaling through platelet factors including TGF β 1 and platelet-derived growth factor, which are known activators of the SMAD and Wnt/ β -catenin pathways, and through specific bioactive phospholipids.^{5,13} The idea that platelets contribute to AS is further supported by histological observations of platelet adhesion directly to aortic VECs in hyperlipidemic mice that develop modest valve thickening and in humans with AS.^{12,13}

We evaluated hyperlipidemic mice deficient for *LDLR* fed a WSD that not only develop atherosclerosis but also have increased endothelial-associated vWF and adhesion of platelets to the arterial wall.^{8,12} The additional genetic deletion of *ADAMTS13* in these mice has been shown to markedly increase vWF-mediated platelet adhesion in the aorta and the development of large vessel atherosclerosis.^{8,9} In the current study, *LDLR*^{-/-}*AD13*^{-/-} mice on WSD demonstrated extensive vWF not only in atherosclerotic lesions, but also on VECs. Most of these mice developed severe thickening of the aortic leaflets with increased transvalvular gradients in the traditionally stenotic range, representing a true model of AS, despite being studied at less than one-half the average lifespan of the background strain. The net increase in afterload from valve stenosis and arterial stiffness in *LDLR*^{-/-}*AD13*^{-/-} mice was reflected by substantial elevations in valvulo-aortic impedance. As a consequence, these mice demonstrated afterload-related reduction in LV function. The high cardiac work index in *LDLR*^{-/-}*AD13*^{-/-} mice indicated that mice were not in a decompensated state and that the decreases in LV function were all secondary to increased afterload. Accordingly, we believe that the hemodynamic measurements that account for differences in load-dependent stroke volume (eg, valve

resistance) best reflect the true extent of AS in *LDLR*^{-/-}*AD13*^{-/-} mice.

Our findings provide firm evidence that failure of ADAMTS13 cleavage of vWF predisposes to AS in a multifactorial way. In animal models of hyperlipidemia, vWF-mediated platelet adhesion is known to accelerate atherosclerosis and to promote the recruitment of cells of the innate immune system to areas of plaque formation.^{5,8,9} Accordingly, the increase in aortic root plaque formation seen in *LDLR*^{-/-}*AD13*^{-/-} mice was not unexpected and, in many cases, there appeared to be an extension of plaque onto the valve leaflet surface. Yet, most of the valve thickening in *LDLR*^{-/-}*AD13*^{-/-} mice was attributable not to inflammatory plaque formation, but rather to extensive proliferation of VICs with evidence for myofibroblastic and osteogenic transformation, an expansion of collagen-rich matrix, MMP-9 up-regulation, and microcalcification.

We believe that deficiency of ADAMTS13 exerted its effects on the aortic valve through enhanced vWF-mediated adhesion of platelets and PMVs. This assumption is reasonable based on mechanistic studies on the effects of ADAMTS13 activity on platelet adhesion in atherosclerosis^{8,9} and on our findings of colocalization of platelet adhesion and signaling pathways known to result in VIC myofibroblastic transformation. Platelet-derived factors, including TGFβ1, can induce VIC myofibroblastic transformation and osteogenic differentiation.^{10,11,27} Although TGFβ1 can originate from a variety of vascular cell types,²⁸ platelet-specific deletion of TGFβ1 has recently been shown to reduce myofibroblastic VICs.¹² We provided evidence for TGFβ1 signaling by histological examination for 2 separate markers, including pSMAD2, which has been associated with valve fibrosis and is even found in platelets,^{12,26,29} and β-catenin, which in some, but not all, studies has been linked to valve thickening and osteogenic signaling.^{19,26,30} We observed a clear increase in both pSMAD2 and β-catenin in *LDLR*^{-/-}*AD13*^{-/-} mice, which was particularly prominent in VECs and VICs that were in close proximity to platelet and PMV adhesion, suggesting juxtacrine signaling. Adherent platelets were also frequently positive for pSMAD2, consistent with studies that have defined the role of TGFβ1 in platelet activation.³¹ These findings highlight the accepted concept that events on the valve surface can influence VICs and valve matrix on the interior through paracrine signaling.³² It should also be noted that TGFβ1 can also cause mesenchymal transformation of VECs with subsequent expression of αSMA.³³ We did not attempt to correlate the degree of platelet adhesion with the degree of leaflet

thickening in *LDLR*^{-/-}*AD13*^{-/-} mice based on the notion that leaflet thickening is a process that occurs over a long timespan, whereas histological evidence for platelet adhesion represents a single snapshot in time. *LDLR*^{-/-}*AD13*^{-/-} mice tended to have higher platelet counts, which may have contributed further to platelet-mediated valve changes. This finding also argues against a thrombotic thrombocytopenic state, which usually requires some triggering stimulus in this strain.

With respect to clinical implications, it is possible that endothelial vWF-related events that predispose to aortic valve disease can be modified by drug therapy. Although antiplatelet therapies traditionally used in atherosclerosis can reduce platelet activation-related signaling, their effect has not been rigorously tested in native valve disease, and they are largely used to inhibit aggregation and not adhesion through interaction between vWF and GPIIb/IIIa. The pathways we have defined can be linked to bleeding tendency in patients with severe AS (Heyde's syndrome) that occurs from loss of ultralarge vWF multimers through valve shear-dependent exposure of the A2 cleavage site.³⁴ Similar shear-dependent conformational changes exposes the A1 binding site for platelet GPIIb/IIIa, thereby representing a mechanism for transition from mild to severe stenosis. It has been reported that proatherogenic abnormalities in cholesterol metabolism can impair vWF proteolysis,³⁵ which may partially explain the excess endothelial-associated vWF and arterial platelet adhesion in hyperlipidemic animals.⁸ Hence, our findings provide additional nonatherosclerotic mechanisms for the association between dyslipidemia and AS.³⁶

STUDY LIMITATIONS. There are limitations of the study in addition to those mentioned in the previous text that deserve mention. First, we have not yet performed interventional studies examining whether inhibiting GPIIb/IIIa-vWF interaction suppresses AS development. Our study design was not intended to provide a comprehensive evaluation of all potential signaling pathways through which vWF-mediated platelet adhesion can act. Instead, we focused on TGFβ1 based on the strength of evidence for its role in AS and its role as a major platelet signaling pathway. It should be also mentioned that when evaluating abnormal aortic valve gradients, it was not possible to separate the relative contributions of valve thickening and aortic root plaque. It could be argued that *LDLR*^{-/-} mice on a chow diet would have also been an appropriate control group to study. Although this group was not prospectively included in our study design, we have generated data from a small number

(n = 4) of age-matched *LDLR*^{-/-} mice on chow diet that indicate that they are similar to wild-type mice, with very little endothelial vWF and platelet adhesion on molecular imaging at 30 weeks, normal blood pressures, and no evidence for aortic valve disease on echocardiography at 50 weeks. Finally, we did not study mice at a more advanced age when strain-related differences may have been even more exaggerated.

CONCLUSIONS

Our data indicate that excess endothelial surface-associated vWF on the aortic leaflets leads to platelet adhesion, accelerated valve thickening, and AS at an advanced age, with secondary afterload-related changes in LV function. The valvular abnormalities that are associated with vWF-mediated platelet adhesion are multifaceted, involving altered matrix collagen, proliferation VICs, VIC myofibroblastic and osteogenic transformation, and to a lesser extent, inflammatory changes. These findings will likely stimulate new investigation into new approaches for mitigating progression of AS.

FUNDING SUPPORT AND AUTHOR DISCLOSURES

Study protocols were supported by the Oregon Health & Sciences University Multiscale Microscopy Core and the Oregon National Primate Research Center Integrative Pathology Core. Dr Ozawa is supported by fellowship grants from the Japanese Society for the

Promotion of Research, the Manpei Suzuki Diabetes Foundation, and the Japanese Society of Echocardiography. Dr López is supported by grant R35-HL145262 from the National Institutes of Health. Dr Lindner is supported by grants R01-HL078610, R01-HL130046, and P51-OD011092 from the U.S. National Institutes of Health; and grant 18-18HCFBP-2-0009 from the U.S. National Aeronautics and Space Administration. All other authors have reported that they have no relationships relevant to the contents of this paper to disclose.

ADDRESS FOR CORRESPONDENCE: Dr Jonathan R. Lindner, Cardiovascular Division, UHN-62, Oregon Health & Science University, 3181 SW Sam Jackson Park Road, Portland, Oregon 97239, USA. E-mail: lindnerj@ohsu.edu. Twitter: [@JLindnerMD](https://twitter.com/JLindnerMD).

PERSPECTIVES

COMPETENCY OF MEDICAL KNOWLEDGE: AS involves the activation and transformation of VICs and possibly VECs, resulting in alteration of the valve matrix and calcification. Platelets are capable of triggering these processes through platelet-derived growth factors and cytokines.

TRANSLATIONAL OUTLOOK: Excess vWF on the valve endothelial surface can promote the adhesion of platelet and secondary paracrine signaling, representing a potential therapeutic target to prevent the progression from aortic sclerosis to AS.

REFERENCES

1. Towler DA. Molecular and cellular aspects of calcific aortic valve disease. *Circ Res*. 2013;113:198-208.
2. Lerman DA, Prasad S, Alotti N. Calcific aortic valve disease: molecular mechanisms and therapeutic approaches. *Eur Cardiol*. 2015;10:108-112.
3. Dimitrow PP, Hlawaty M, Undas A, et al. Effect of aortic valve stenosis on haemostasis is independent from vascular atherosclerotic burden. *Atherosclerosis*. 2009;204:e103-e108.
4. Weber C. Platelets and chemokines in atherosclerosis: partners in crime. *Circ Res*. 2005;96:612-616.
5. Rondina MT, Weyrich AS, Zimmerman GA. Platelets as cellular effectors of inflammation in vascular diseases. *Circ Res*. 2013;112:1506-1519.
6. Wu MD, Atkinson TM, Lindner JR. Platelets and von Willebrand factor in atherogenesis. *Blood*. 2017;129:1415-1419.
7. Rolfes V, Ribeiro LS, Hawwari I, et al. Platelets fuel the inflammasome activation of innate immune cells. *Cell Rep*. 2020;31:107615.
8. Ozawa K, Muller MA, Vartanov O, et al. Proteolysis of von Willebrand factor influences endothelial activation and vascular compliance in atherosclerosis. *J Am Coll Cardiol Basic Trans Science*. 2020;5:1017-1028.
9. Gandhi C, Ahmad A, Wilson KM, Chauhan AK. ADAMTS13 modulates atherosclerotic plaque progression in mice via a VWF-dependent mechanism. *J Thromb Haemost*. 2014;12:255-260.
10. Rutkovskiy A, Malashicheva A, Sullivan G, et al. Valve interstitial cells: the key to understanding the pathophysiology of heart valve calcification. *J Am Heart Assoc*. 2017;6(9):e006339. <https://doi.org/10.1161/JAHA.117.006339>
11. Liu AC, Joag VR, Gottlieb AI. The emerging role of valve interstitial cell phenotypes in regulating heart valve pathobiology. *Am J Pathol*. 2007;171:1407-1418.
12. Varshney R, Murphy B, Woolington S, et al. Inactivation of platelet-derived TGF-beta1 attenuates aortic stenosis progression in a robust murine model. *Blood Adv*. 2019;3:777-788.
13. Bouchareb R, Boulanger MC, Tastet L, et al. Activated platelets promote an osteogenic programme and the progression of calcific aortic valve stenosis. *Eur Heart J*. 2019;40:1362-1373.
14. Ruggeri ZM. Von Willebrand factor, platelets and endothelial cell interactions. *J Thromb Haemost*. 2003;1:1335-1342.
15. Shim CY, Liu YN, Atkinson T, et al. Molecular imaging of platelet-endothelial interactions and endothelial von Willebrand factor in early and mid-stage atherosclerosis. *Circ Cardiovasc Imaging*. 2015;8:e002765.
16. Moccetti F, Brown E, Xie A, et al. Myocardial infarction produces sustained proinflammatory endothelial activation in remote arteries. *J Am Coll Cardiol*. 2018;72:1015-1026.
17. Borlaug BA, Kass DA. Ventricular-vascular interaction in heart failure. *Heart Fail Clin*. 2008;4:23-36.
18. Bogdanova M, Zabinnyk A, Malashicheva A, et al. Interstitial cells in calcified aortic valves have reduced differentiation potential and stem cell-like properties. *Sci Rep*. 2019;9:12934.
19. Chen JH, Chen WL, Sider KL, Yip CY, Simmons CA. beta-catenin mediates mechanically regulated, transforming growth factor-beta1-induced myofibroblast differentiation of aortic valve interstitial cells. *Arterioscler Thromb Vasc Biol*. 2011;31:590-597.
20. Satta J, Oiva J, Salo T, et al. Evidence for an altered balance between matrix metalloproteinase-9 and its inhibitors in calcific

aortic stenosis. *Ann Thorac Surg.* 2003;76:681-688. discussion 688.

21. Poggio P, Branchetti E, Grau JB, et al. Osteopontin-CD44v6 interaction mediates calcium deposition via phospho-Akt in valve interstitial cells from patients with noncalcified aortic valve sclerosis. *Arterioscler Thromb Vasc Biol.* 2014;34:2086-2094.

22. Dong JF, Moake JL, Nolasco L, et al. ADAMTS-13 rapidly cleaves newly secreted ultralarge von Willebrand factor multimers on the endothelial surface under flowing conditions. *Blood.* 2002;100:4033-4039.

23. Shankaran H, Alexandridis P, Neelamegham S. Aspects of hydrodynamic shear regulating shear-induced platelet activation and self-association of von Willebrand factor in suspension. *Blood.* 2003;101:2637-2645.

24. Chen J, Fu X, Wang Y, et al. Oxidative modification of von Willebrand factor by neutrophil oxidants inhibits its cleavage by ADAMTS13. *Blood.* 2010;115:706-712.

25. Li Z, Delaney MK, O'Brien KA, Du X. Signaling during platelet adhesion and activation. *Arterioscler Thromb Vasc Biol.* 2010;30:2341-2349.

26. Miller JD, Weiss RM, Serrano KM, et al. Evidence for active regulation of pro-osteogenic

signaling in advanced aortic valve disease. *Arterioscler Thromb Vasc Biol.* 2010;30:2482-2486.

27. Osman L, Yacoub MH, Latif N, Amrani M, Chester AH. Role of human valve interstitial cells in valve calcification and their response to atorvastatin. *Circulation.* 2006;114:1547-1552.

28. Chen PY, Qin L, Li G, et al. Endothelial TGF-beta signalling drives vascular inflammation and atherosclerosis. *Nat Metab.* 2019;1:912-926.

29. Miller JD, Weiss RM, Serrano KM, et al. Lowering plasma cholesterol levels halts progression of aortic valve disease in mice. *Circulation.* 2009;119:2693-2701.

30. Jenke A, Kistner J, Saradar S, et al. Transforming growth factor-beta1 promotes fibrosis but attenuates calcification of valvular tissue applied as a three-dimensional calcific aortic valve disease model. *Am J Physiol Heart Circ Physiol.* 2020;319:H1123-H1141.

31. Lev PR, Salim JP, Marta RF, Osorio MJ, Goette NP, Molinas FC. Platelets possess functional TGF-beta receptors and Smad2 protein. *Platelets.* 2007;18:35-42.

32. Gould ST, Matherly EE, Smith JN, Heistad DD, Anseth KS. The role of valvular endothelial cell paracrine signaling and matrix elasticity on

valvular interstitial cell activation. *Biomaterials.* 2014;35:3596-3606.

33. Hjortnaes J, Shapero K, Goettsch C, et al. Valvular interstitial cells suppress calcification of valvular endothelial cells. *Atherosclerosis.* 2015;242:251-260.

34. Vincentelli A, Susen S, Le Tourneau T, et al. Acquired von Willebrand syndrome in aortic stenosis. *N Engl J Med.* 2003;349:343-349.

35. Chung DW, Chen J, Ling M, et al. High-density lipoprotein modulates thrombosis by preventing von Willebrand factor self-association and subsequent platelet adhesion. *Blood.* 2016;127:637-645.

36. Cote C, Pibarot P, Despres JP, et al. Association between circulating oxidised low-density lipoprotein and fibrocalcific remodelling of the aortic valve in aortic stenosis. *Heart.* 2008;94:1175-1180.

KEY WORDS aortic valve stenosis, echocardiography, von Willebrand factor

APPENDIX For an expanded Methods section as well as supplemental figures and a table, please see the online version of this paper.